Mon. Not. R. astr. Soc. (1986) **221,** 823–838

A multi-wavelength study of the long-period AM Her system E2003+225 – I. The soft X-ray light curve and overall energy spectrum

J. P. Osborne,[1,2] J.-M. Bonnet-Bidaud,[3] S. Bowyer,[4] P. A. Charles,[5] L. Chiappetti,[6] J. T. Clarke,[7] J. P. Henry,[8] G. J. Hill,[8] S. Kahn,[4] L. Maraschi,[9] K. Mukai,[5] A. Treves[9] and S. Vrtilek[10]

[1] *EXOSAT Observatory, ESOC, Robert Bosch Strasse 5, 6100 Darmstadt, Federal Republic of Germany*
[2] *Affiliated to Astrophysics Division, Space Science Department of ESA*
[3] *CEN-Saclay, Dph/SAP, 91191 Gif-sur-Yvette Cedex, France*
[4] *Space Science Laboratory, University of California, Berkeley, California 94720, USA*
[5] *Department of Astrophysics, University of Oxford, South Parks Road, Oxford OX1 3RQ*
[6] *Instituto di Fisica Cosmica, CNR, Via Bassini 15, 20131 Milano, Italy*
[7] *Space Telescope Project Office, Marshall Space Flight Center, Alabama 35812, USA*
[8] *Institute for Astronomy, University of Hawaii, 2680 Woodland Drive, Honolulu, Hawaii 96822, USA*
[9] *Dipartimento di Fisica, Università di Milano, Via Celoria 16, 20133 Milano, Italy*
[10] *Columbia Astrophysics Laboratory, Columbia University, 538 West 120th Street, New York, New York 10227, USA*

Accepted 1986 March 16. Received 1986 March 13; in original form 1985 December 5

Summary. We present X-ray, UV and optical observations of the longest period AM Her object E2003+225 from 1983 October 12, together with a new linear polarization ephemeris. The optical and X-ray data were obtained simultaneously and the UV observations were carried out on the same day. A 6-hr observation with the *EXOSAT* 500 line mm^{-1} objective grating restricts soft X-ray blackbody temperatures to the range 18–29 eV. The blackbody luminosity exceeds the hard X-ray luminosity by at least a factor of 4.5, but is of the same order as the optical/UV component. The soft X-ray (0.1–0.25 keV) and hard X-ray (1–6 keV) light curves covering almost two orbital periods are presented. The soft X-ray light curve shows two broad maxima and two eclipses per orbital period, the second eclipse coincides with a deep minimum of the equivalent widths of the low-ionization optical emission lines. The X-ray light curves are not easily explained by current theoretical work. No soft X-ray spectral variation is seen, so we believe that photoelectric absorption does not play a major role in the

formation of the soft X-ray light curve apart from the eclipses. These eclipses are interpreted as being due to different parts of the magnetically confined accretion stream.

1 Introduction

E2003+225 was discovered with the *HEAO-1* low-energy detectors and catalogued as H2005+22 (Nugent *et al.* 1983). A more accurate position was obtained with *Einstein* IPC observations. These led to the optical identification and to the recognition of its AM Her like nature (Nousek *et al.* 1982). The *HEAO-1* and the *Einstein* observations, optical spectroscopy, photometry and polarimetry obtained in 1982 are described in detail in Nousek *et al.* (1984, hereafter N84), who derive a geometry for the system that has the accreting pole almost continuously in view. They also obtain an orbital period of 3.71 hr, making this the longest period AM Her system known. Archive plate photometry by Andronov & Yavorskii (1983) covering the interval 1962–82 shows that E2003+225 is normally a 15th magnitude object, having occasional fainter episodes, but none brighter. The optical counterpart has recently been named QQ Vul (Kholopov *et al.* 1985).

Our current understanding of AM Her objects in general has been reviewed by Liebert & Stockman (1985) and Lamb (1985). Much attention has been given to the issue of the so called 'soft X-ray puzzle'. This has arisen from the theoretical expectation that the luminosity in the cyclotron and hard X-ray thermal bremsstrahlung components would be comparable to that in soft X-rays, which are thought to be due to thermalization of these other two components. Observations of some sources have led to the suggestion that the soft X-ray luminosity greatly exceeds that of the other components; however, a reliable determination of the blackbody and cyclotron luminosities is very difficult.

Here we report on optical, UV and X-ray observations of E2003+225 obtained on 1983 October 12. The source was observed continuously for over 6 hr with the *EXOSAT* satellite, resulting in a high-quality soft X-ray light curve and an objecting grating soft X-ray spectrum. E2003+225 was seen as a weak source by the medium-energy experiment (Section 3.1), and this constitutes the first detection of this source above 1 keV. Simultaneous optical spectrophotometry was performed on Mauna Kea and spectra were also taken at Lick (Section 3.2). Far-UV spectra were obtained with *IUE* 12 hr after the X-ray observations (Section 3.3). These are the first UV observations of E2003+225 to be reported. In Section 4 the soft and hard X-ray light curves are discussed with reference to existing models, and the origin of the observed eclipses is considered. The overall continuum spectrum is then discussed, with emphasis on the relative luminosities of the various spectral components.

The accompanying paper (Mukai *et al.* 1986, Paper II) reports on observations of E2003+225 made in 1984 July and focuses on changes in the system parameters. Both this paper and Paper 2 use the refined linear polarization ephemeris derived in Section 2 of this paper.

2 Linear polarization ephemeris

We have redetermined the linear polarization ephemeris of E2003+225 using the seven pulse times used by N84 (Tapia 1985, private communication) together with the one time and the one phase available in Cropper (1985). These data are listed in Table 1. We used a least-squares fitting technique to determine the period and epoch and their errors. A formal fit for a single period could not be achieved given the timing errors for Tapia's data alone, indicating that small (~0.02) phase differences are common. By increasing the timing uncertainties we achieved a good fit for a single period. Cropper's data are consistent with this intermediate ephemeris (based only on

Table 1. Linear polarization pulse times.

HJD	error(sec)	E	O-C(phase)
2445234.83952	120	0	.0201
2445254.76888	120	129	-.0054
2445255.69073	120	135	-.0395
2445316.58052	300	529	.0140
2445318.58528	180	542	-.0121
2445464.92218	60	1489	.0196
2445468.94067	60	1515	.0257
2445533.52481[a]	180	1933	-.0124
2445852.14346[a,b]	666	3995	-.0448

All times from Tapia (1985, private communication), except[a] from Cropper (1985).[b] This point calculated from the phase of a very weak pulse in a folded light curve of 2.4 cycles taken during 1984 May 30–June 1.

Tapia's data). All the data were then included in the fitting process, the errors were evaluated at $\chi^2_{\min}+2.3$ and correspond to 68 per cent confidence. The resulting linear polarization ephemeris is

$$\text{HJD } 2445234.8364(\pm 18) + 0.1545217(\pm 22)\,E.$$

We use this ephemeris throughout this paper and Paper II. It is evident that N84 overestimated the precision of their ephemeris.

3 Observations

3.1 X-RAYS

EXOSAT observed E2003+225 for over 6 hr starting at 0259 UT, 1983 October 12. A log of the observation is given in Table 2. Both low-energy telescopes (LE1, LE2) were available, the 500 line mm^{-1} grating in LE2 was used after 0333 UT. The low-energy telescopes were used with the 3000 lexan and the aluminium/parylene filters. Half of the medium-energy (ME) detectors were offset throughout the observation in order to monitor the background. These instruments are described by de Korte *et al.* (1981), and Turner, Smith & Zimmerman (1981) respectively.

The soft X-ray light curve of E2003+225 covering $\sim 1.7\,P_{\rm orb}$ is shown in Fig. 1(a). The source was relatively bright, averaging 26.4 counts per minute through the 3000 lexan filter on LE1. The 500 line mm^{-1} grating was therefore inserted into the beam in LE2 to provide detailed spectral information. The light curve shows two broad minima per cycle at phases 0.35 and 0.65.

A total eclipse is readily apparent, centred on $\phi=0.350$ and total for $\Delta\phi=0.07$. The 2σ upper limit to the count rate during the central 600 s of this event is 7 per cent of the mean. We will call this event the broad X-ray eclipse.

There is another interval during which the source disappears for 41 s centred on $\phi=0.435$. This is part of a broader dip in the soft X-ray light curve some 3 or 10 min long. We will call this the narrow X-ray eclipse, it is shown in Fig. 1(b). During the central 20 s of this eclipse the number of counts seen at the position of E2003+225 is such that it has a Poisson probability of being due solely to the background of 0.08. Thus the source is not detectable at this time. The typical equivalent probabilities in adjacent 20-s time bins are of order 3×10^{-7}. This eclipse is short and only observed with sensitivity on one occasion: we cannot provide a strong upper limit to the count rate during the eclipse because of this. Its appearance of totality may possibly be related to the flickering observed at other phases (~20 per cent variation on time-scales longer than 80 s

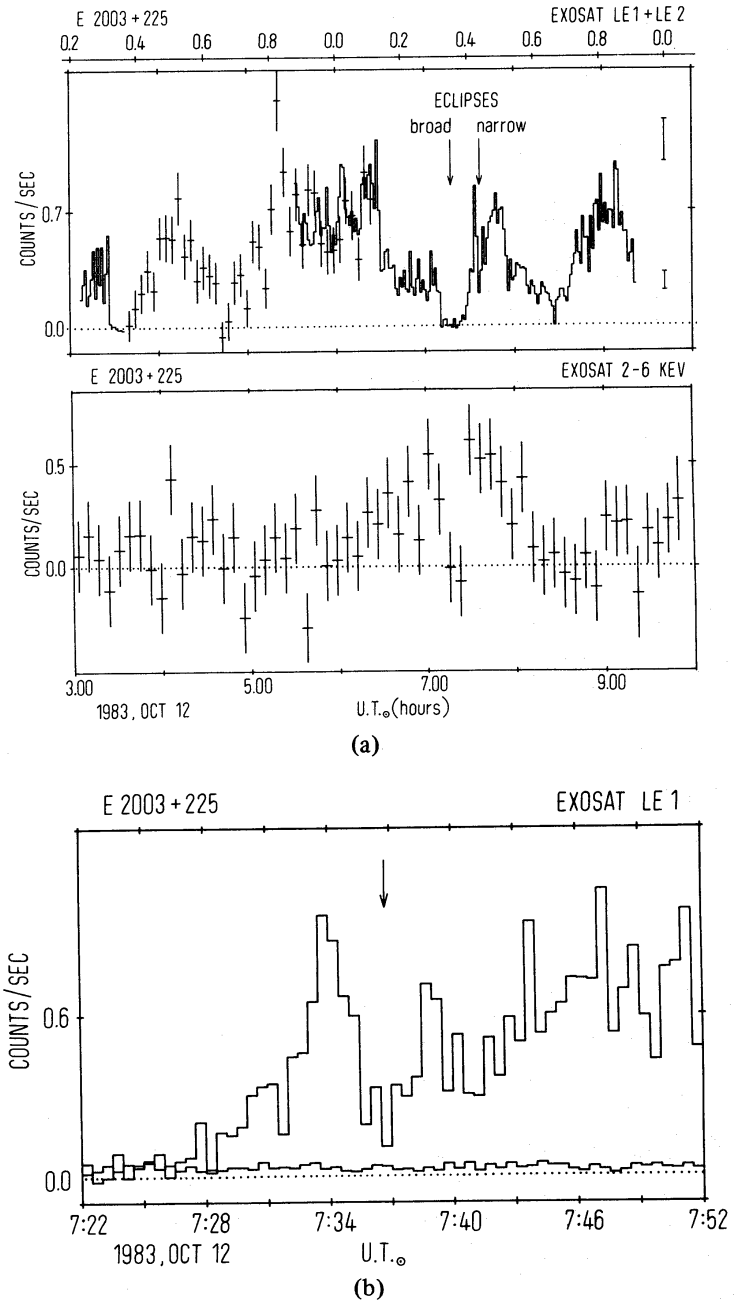

Figure 1. (a) *Top:* The 0.10–0.25 keV X-ray light curve obtained by *EXOSAT*. The histogram shows the LE1+3000 lexan data, the crosses show the LE2+grating+3000 lexan data. The grating light curve was obtained by summation of the zero and ±1st order images. All the grating data were normalized by comparison with the LE1 data, however, only part of the grating light curve is plotted for clarity. Typical $\pm 1\sigma$ errors for the LE1 data are shown on the right. The narrow soft X-ray eclipse at $\phi = 0.435$ does not appear total in the LE1 light curve because it is plotted in 84-s bins. *Bottom:* The simultaneous 2–6 keV X-ray light curve. Linear polarization phase is shown at the top. (b) The background subtracted soft X-ray light curve around the time of the narrow eclipse (arrowed) together with the background count rate. The data are plotted in 30-s bins.

during UT 0530–0630). However, the similarity of the phase widths and the separation of this double eclipse pattern to those seen in AN UMa and E1405−451 (Osborne *et al.* 1984) is very striking.

E2003+225 was also detected by the ME experiment at a mean 2–6 keV count rate of

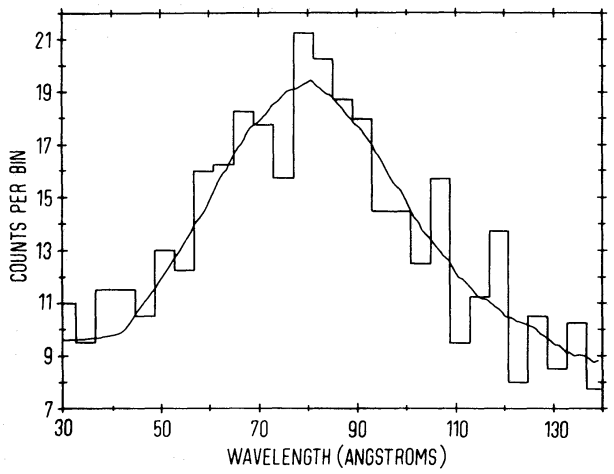

Figure 2. Half of the dispersed count spectrum obtained with the 500 line mm^{-1} grating, together with the best blackbody fit to the source plus background derived simultaneously for both positive and negative orders.

0.15 ± 0.05 counts per second in the four Argon detectors pointed at the source (area $\sim 750\,cm^2$). Background subtraction was performed using the offset half count rate, which was constant, after correction for the observed difference between the halves during the source-free slew periods. The count rate, which is shown together with that from the LE's in Fig. 1(a), shows that the flux drops to zero during the broad soft X-ray eclipse when the source is bright; however, some orbit-to-orbit variation is apparent. The mean count rate corresponds to a flux of $f_{2-6}= 1.5\times10^{-12}\,erg\,cm^{-2}\,s^{-1}$ assuming a thermal bremsstrahlung spectrum with $kT>1$ keV.

E2003+225 was observed with the 500 line mm^{-1} grating in LE2 (resolution FWHM=3.2 Å at 0.18 keV) with the 3000 lexan filter in place for $1.6\,P_{orb}$ (phases 0.35 to 1.92). A spectrum was extracted from the image by summing counts in a 25-pixel wide band. The background was accumulated in six similar bands rotated by $\pm25°$, $\pm50°$ and $\pm75°$ with respect to the dispersion axis. A least-squares fitting procedure was used to fit the data (binned in 4 Å bins) to the model

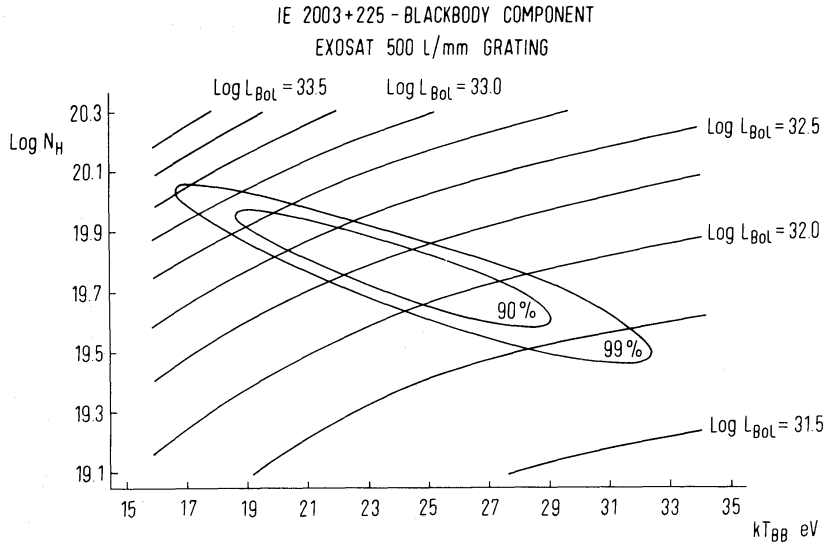

Figure 3. The 90 and 99 per cent confidence regions ($\chi^2_{min}+4.6$ and $\chi^2_{min}+9.2$) for the temperature and absorbing column allowed by the blackbody fits to the LE2 grating data. The bolometric luminosity (for an assumed distance of 100 pc) required to give the average observed count rate is also shown.

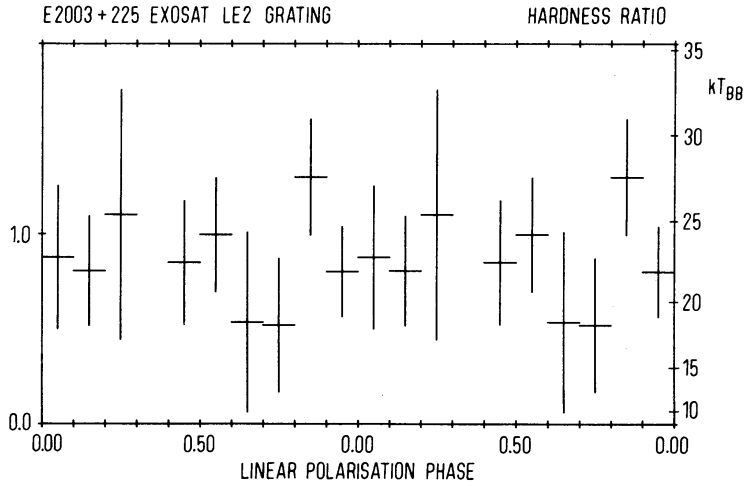

Figure 4. The hardness ratio, (0.15–0.25) keV/(0.10–0.15) keV, as derived from the 500 line mm^{-1} grating data as a function of phase. No significant variation is seen. On the right are shown the blackbody temperatures equivalent to the hardness ratios for $N_H=5.6\times10^{19}\,cm^{-2}$.

spectra folded through the response of the system. Left and right dispersions were fitted simultaneously (but treated separately) using a smoothed and interpolated background. This is similar to the technique described by Cordova, Mason & Kahn (1985).

The source was detected in the energy range 0.10–0.25 keV. No emission or absorption features were seen in the grating spectrum (shown in Fig. 2) and good fits to a blackbody were obtained with $\chi^2_{min}/\nu=57.1/48$ at $kT_{BB}=25$ eV and $N_H=5.6\times10^{19}\,cm^{-2}$. The results of this analysis are illustrated in Fig. 3. The 90 per cent confidence limits are $4\times10^{19}<N_H<10^{20}\,cm^{-2}$, $18<kT<29$ eV. These parameter values are consistent with the 3000 lexan to Al/P count rate ratio measured in the first 30 min of the observation. The mean 0.10–0.25 keV flux detected over one orbital period [after correction for the obscuration due to the over-opened ME flap, the sum signal distribution and the sampling dead time (Osborne 1985)] was $1.1\times10^{-11}\,erg\,cm^{-2}\,s^{-1}$, slightly lower than that measured by N84 with the *Einstein* IPC ($1.4\times10^{-11}\,erg\,cm^{-2}\,s^{-1}$). No significant spectral variation is seen (see Fig. 4) in contrast to the *Einstein* grating observation of AM Her (Heise *et al.* 1984).

Table 2. Log of observations E2003+225.

Observatory	Instrument	λ(Å)	Resolution (Å)	UT Oct 12,1983
EXOSAT	LE1+3Lx	6.5-210	-	03:04-03:34 05:29-09:21
	LE1+Al/P	6.9-95,155-310	-	03:36-05:27
	LE2+Al/P	"	-	03:01-03:25
	LE2+3Lx+grating	6.5-210	3.2	03:33-09:22
	ME	0.6 - 12	-	02:59-09:54
IUE	SWP (21281)	1150-1950	7	15:08-16:59
	LWP (2033)	1900-3000	7	17:12-19:03
	SWP (21282)	1150-1950	7	19:08-21:48
LICK	3m + IDS	4500-6800	8	03:03-03:19
	"	3000-5200	8	03:22-03:38
MAUNA KEA	88" + GRISM+CCD	4300-6050	16	06:08-09:04

3.2 OPTICAL

3.2.1 Spectroscopy

Two 16 min spectra were obtained with the Lick 3-m Shane Telescope and the Image Dissector Scanner (Robinson & Wampler 1972; Miller, Robinson & Wampler 1976) at 8 Å resolution by JTC at the same time as the start of the *EXOSAT* observation (see Table 2 for details). These are shown in Fig. 5. They are corrected for the instrument response by observation of a standard star; however, the sky was not photometric. These spectra imply a mean radial velocity of zero, consistent with the value found in Paper II, but different to that derived from the Mauna Kea spectrophotometry and different to the value given in N84.

3.2.2 Spectrophotometry

Low-resolution spectrophotometric data were obtained with the University of Hawaii 88-inch telescope on Mauna Kea by GJH and JPH between UT 0608 and 0904 1983 October 12, simultaneously with the latter half of the *EXOSAT* observation. The UH grism spectrograph and the Galileo/Institute for Astronomy CCD camera (Hlivak, Henry & Pilcher 1984) were mounted at the Cassegrain focus, giving a dispersion of 270 Å mm^{-1} and a wavelength coverage of 4300 to

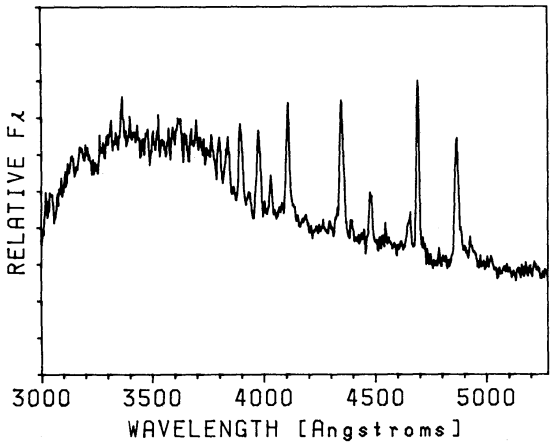

(a)

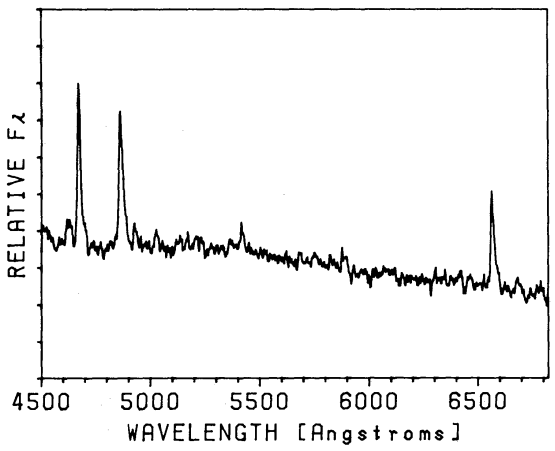

(b)

Figure 5. Blue (a) and red (b) spectra from the Lick observations.

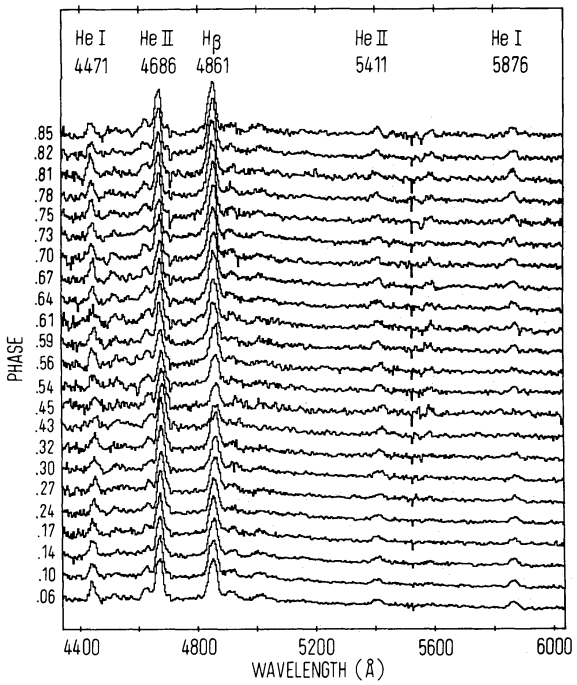

Figure 6. (a) The spectrophotometric data obtained from Mauna Kea. All spectra are normalized to the same intensity and offset uniformly.

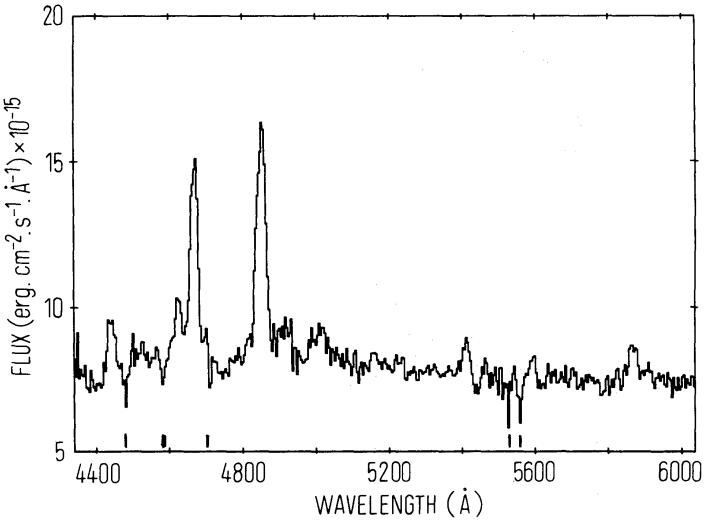

Figure 6. (b) The mean of the spectra shown in Fig. 6(a). Individual spectra have not been wavelength shifted before addition. Non-stellar features are marked.

6050 Å. Five min exposures were taken at approximately 6-min intervals covering phases 0.06 to 0.85. We observed the standard star Feige 15 (Stone 1977) to calibrate the system response. Comparison spectra of a neon lamp, reflected from the dome, were taken to determine the wavelength scale.

The CCD processing was standard. Biases were subtracted and the frames then flattened using dome flats. The lack of any neon lines shortwards of 4700 Å makes the wavelength calibration in this part of the spectrum suspect, a linear extrapolation of the longer wavelength data being adopted for the linearization curve. Longwards of 4700 Å the wavelength scale is well

determined, giving a velocity for the standard star of $+25\,\mathrm{km\,s^{-1}}$. The entire data set is shown in Fig. 6(a), in which photometric changes have been removed by dividing each spectrum by the total flux in that spectrum. The mean spectrum is shown in Fig. 6(b).

The *B* and *V* magnitudes which result from folding the spectra through the standard filter

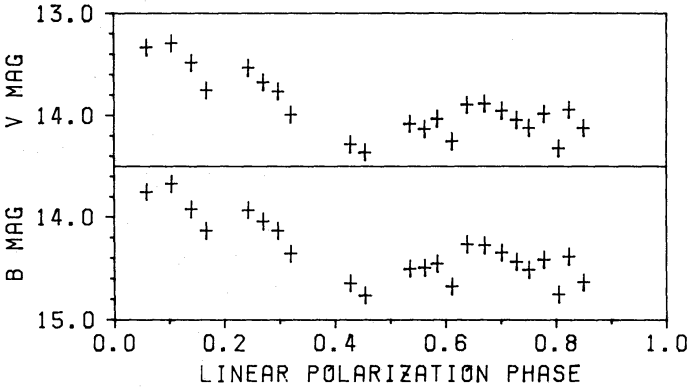

Figure 7. *B* and *V* magnitudes, obtained by folding the spectra with the standard filter response functions, are plotted against linear polarization phase. These data were obtained simultaneously with the latter half of the *EXOSAT* data.

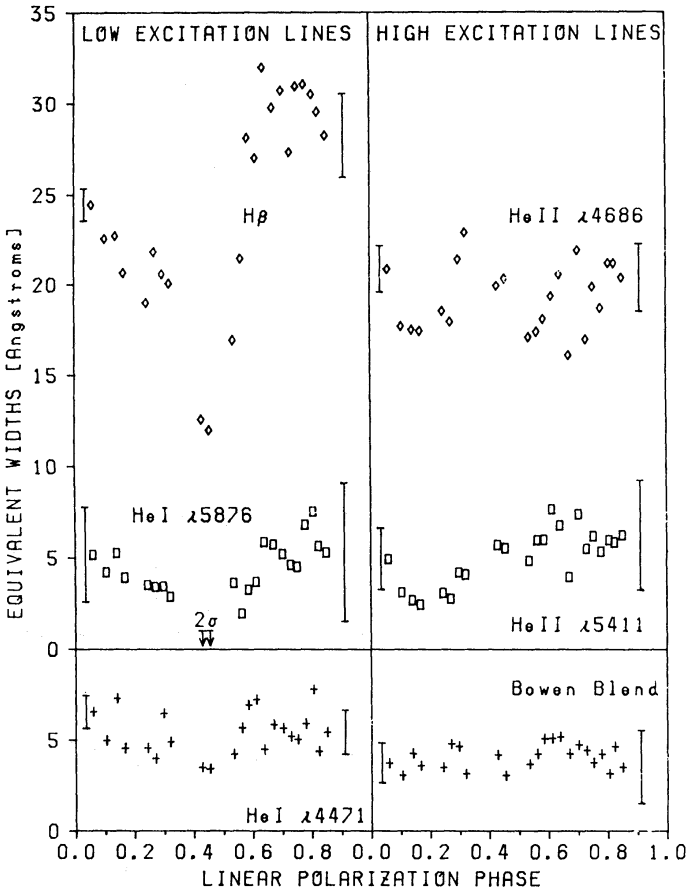

Figure 8. Equivalent widths of six major emission lines are plotted against phase. Typical $\pm 1\sigma$ errors are shown for the beginning and the end of the observations; the difference is due to the decline in brightness. We have divided the lines into 'low-excitation lines' and 'high-excitation lines', each of which is subdivided into two panels for clarity. Hβ shows a clear eclipse between phases 0.4 and 0.5; for He I 4471 Å, the evidence is marginal; for He I 5876 Å, we could not detect the line during this phase (indicated by the arrows), although the statistics are poor. High-excitation lines, on the other hand, show *no* sign of eclipse.

transmission curves are plotted as a function of linear polarization phase in Fig. 7. These data show that, compared to 1982 September (N84), E2003+225 was 0.8 mag brighter in blue light until phase 0.5, with the difference decreasing to 0.3 mag by the end of our observation. This difference is greater in the *V* band. Apart from this, the form of the light curves is similar to those of N84.

The archive plate study of Andronov & Yavorskii (1983) does not show E2003+225 to have been brighter than 15 mag during 1962–82. We have thus observed it in an unusual optically bright state, in spite of the fact that the soft X-ray flux was not larger than in previous observations.

The equivalent widths of the major emission lines are plotted as a function of phase in Fig. 8. Significant variations are seen in all major lines, but for some these are probably not more than flickering. Hβ shows a large equivalent width peak during the phase interval 0.6–0.9, and a dramatic dip centred on phase 0.44. This dip is coincident with, but somewhat longer than, the narrow soft X-ray eclipse. The He I 5876 Å line becomes undetectably faint at this time, and the He I 4471 Å line also has minimum equivalent width here. None of the high-excitation lines (He II 4686 Å, He II 5411 Å, C/N blend 4640 Å) show this behaviour.

The low resolution of these spectra make a detailed radial velocity study difficult. However, we can state that the mean velocity is not consistent with that observed by N84 in 1982 July–August, nor is it consistent with the Lick spectroscopy taken ~5 hr previously. Our data imply a mean velocity of $-350\pm100\,\mathrm{km\,s^{-1}}$ for the reliably calibrated Hβ, H II 5411 and H I 5876 Å lines. The

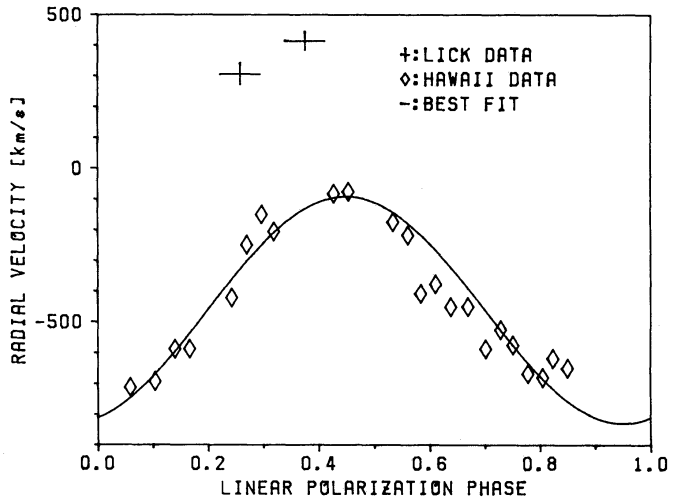

Figure 9. Radial velocities of Hβ from the Mauna Kea spectra are plotted against linear polarization phase, together with the best-fit sinusoid. Also shown are the two points from the Lick observations, which were taken during the previous orbital cycle.

Table 3. Radial velocities derived from the Mauna Kea data.

$$V = \gamma + k \sin(2\pi(\phi-\phi_o))$$

	γ km.s^{-1}	k km.s^{-1}	ϕ_o
He I 5876	-400	250	0.20
He II 5411	-170	400	0.20
Hβ	-460	369	0.20

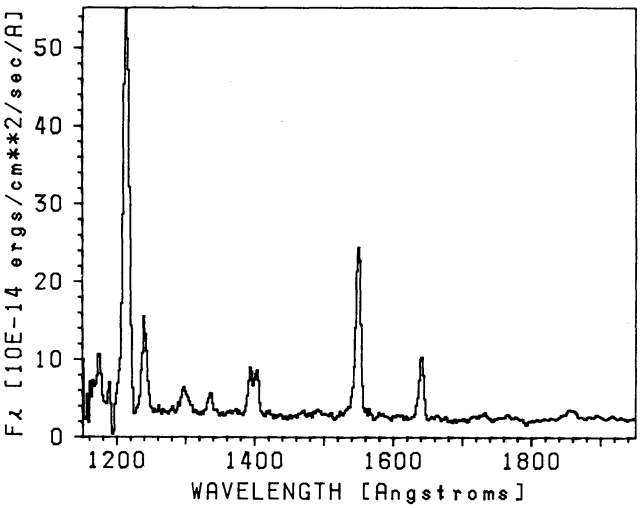

Figure 10. The average of the two SWP spectra taken on 1983 October 12.

Table 4. UV emission-line equivalent widths and intensities.

ID	OBS WAVELENGTH Å	E.W. Å	INTENSITY 10^{-14}erg.cm^{-2}.s^{-1}
N V	1240.8	30±2	103
Si III or O I	1298.9	10±3	36
C II	1336.3	6±1	17
S IV	1398.6	31±5	81
C IV	1550.0	58±10	200
He II	1641.1	19±7	67

Table 5. Mean UV continuum intensities.

WAVELENGTH (Å)	FLUX (10^{-14}erg.cm^{-2}.s^{-1}.Å^{-1})
1480	3.06±0.06
1770	2.45±0.07
2700	1.41±0.02

amplitude of the radial velocity variation is consistent with that of N84 and Paper II, although there appears to have been a shift to later phases between mid 1982 and 1983 October. Details are given in Table 3. The radial velocity curve of Hβ is shown in Fig. 9, together with the Lick measurements. Changes in the radial velocity curve of E2003+225 are discussed in Paper II.

3.3 ULTRAVIOLET

E2003+225 was observed by JMB-B on 1983 October 12, with *IUE*. The observing log is given in Table 2, all exposures were made at least half an orbital period long to obtain good continuum

Table 6. UV spectral-fit results.

SPECTRUM	E(B-V)	α^* or T(K)	χ^2_{red}	f(1200-3200Å) 10^{-11}erg.cm^{-2}.s^{-1}
Power Law	0.0	1.29	4.0	4.14
	0.1	1.63	5.4	8.40
Blackbody	0.0	19500	4.3	4.05
	0.1	21300	4.5	8.10

* $F_\lambda = A\lambda^{-\alpha}$

exposures. The mean SWP spectrum is shown in Fig. 10. These are the first UV spectra reported for this object. The emission-line intensities and the equivalent widths are listed in Table 4; continuum intensities are listed in Table 5. There is no significant change in the lines nor in the continuum between the two SWP spectra, which were taken one orbital cycle apart. An upper limit of 0.1 on $E(B-V)$ can be deduced from the LWP spectrum by setting a limit on the 2200 Å absorption feature assuming a standard galactic extinction law.

The continuum intensities in 50 and 100 Å wide line-free regions have been fitted with power-law and blackbody spectra. The results of this work are summarized in Table 6. Blackbody fits show a short-wavelength excess which is of the same order as the extrapolated soft X-ray blackbody spectrum for $kT \sim 18$ eV. The shape of the excess is *not* matched by such a blackbody spectrum though. The power-law spectrum does not extrapolate smoothly to the mean optical spectrum from the Mauna Kea observations, however, these were not simultaneous.

4 Discussion

4.1 THE X-RAY LIGHT CURVE

The soft X-ray light curve of E2003+225 (Fig. 1a) poses several interesting problems. Its shape is rather complicated, far from that which would be expected from the varying aspect of the hot polar cap at the base of the accretion column (Imamura & Durisen 1983). On the other hand, it is rather similar to those of E1405−451 and AN UMa (Osborne *et al.* 1984), indicating that the problem is not restricted to this one object. The overall form of the light curve presented here is similar to that seen by the *Einstein* IPC in 1981 (N84). There is, however, weak evidence (2.3σ) for a shift in the phase of the X-ray eclipse from $\phi = 0.20 \pm 0.05$ in 1981 April to $\phi = 0.35 \pm 0.04$ in 1983 October. (As stated in Section 2, all phases in this paper refer to the linear polarization ephemeris derived in that section.)

From Paper II it is evident that the optical minimum occurs ~0.1 orbital periods before the emission-line eclipses. If the same relative phasing applies to the observations described here, then the optical minimum occurs at the same time as the broad X-ray eclipse. (This is difficult to verify directly from our data due to the poor time resolution.) N84 have shown that the circular polarization changes rapidly to become zero for $0.06 P_{orb}$ before returning to its previous behaviour, this 'glitch' occurs at the same phase as the optical minimum. Thus the optical minimum, broad X-ray eclipse and circular polarization glitch occur simultaneously and most probably have a common origin.

The polarization and radial velocity data suggest that the axis of the accretion column is not far

from the line-of-sight at the time of the broad eclipse. Although the eclipse could be attributed to the secondary in this particular system, the similarity of the soft X-ray light curve of E2003+225 with those of AN UMa and E1405−451 and the relatively small depth of the optical minimum (compared with the case of E1114+182 which shows an eclipse depth of >4 mag due to the companion, Biermann *et al.* 1985) rather suggest an eclipse of the region close to the white dwarf surface by the distant accretion stream. With the geometry derived by N84, such an eclipse must occur. The ME light curve implies that the matter has a column density greater than 7×10^{22} cm^{-2}, consistent with the simple theoretical estimate of King & Williams (1985).

The duration of the eclipse can be used to derive an upper limit to the size of the accreting region as follows. The part of the column responsible for the eclipse must be rising above the orbital plane. According to Liebert & Stockman (1985) the magnetic field of the white dwarf controls the flow at $R_M > R > R_{WD}$, where the magnetospheric radius R_M is $\sim 30\,R_{WD}$. If the column at $R = 20\,R_{WD}$ (i.e. that part rising out of the orbital plane) has an angular size of 25°, as is implied by the observed broad eclipse width, then tracing the field lines down to the white dwarf surface yields a fractional accreting area of $\sim 10^{-4}$, similar to the results of our grating observation (see Section 4.2). This is an upper limit because our line-of-sight probably does not cross the accretion stream at 90°.

It is also conceivable that this form of eclipse should be associated with the narrow soft X-ray eclipse seen at $\phi = 0.435$. However, this leaves us without a reasonable explanation for the broad X-ray eclipse. The narrow X-ray eclipse is more probably due to a self-eclipse of the accretion region by material on the magnetic axis deep in the accretion column. Such an event would be expected in this system to follow the eclipse by the distant accretion stream and to occur close to phase 0.5. The narrow nature of this eclipse and its association with an eclipse of the low-ionization emission lines remain unexplained.

The overall form of the soft X-ray light curve was expected to be essentially sinusoidal with a maximum when the accreting pole is closest to face-on (Imamura & Durisen 1983). We take this to be at linear polarization phase ~0.45 on the basis of the phase of the radial velocity variation of the emission lines. Photoelectric absorption is not responsible for the difference between the observed and predicted light curves. If it were, absorption by $\sim 6\times10^{19}$ cm^{-2} of cold matter would be required between phases ~0.2 to ~0.7. This would increase the hardness (see caption, Fig. 4) of the escaping radiation by a factor of 2.8. Fig. 4 shows clearly that such an increase does not occur. Moreover, the observed column density is probably entirely interstellar, as the average interstellar absorption in the direction of E2003+225 (Paresce 1984) implies a higher column density than observed if the distance is greater than ~100 pc.

We have considered the possibility that material deep in the accretion column, above the shock, may cause partial obscuration (i.e. total absorption, $N_H > 5\times10^{20}$) of the soft X-ray emitting spot when it is observed near to face-on. In this case it would be possible to understand the soft X-ray light curve as due to a single pole with maximum aspect at phase ~0.45, but two thirds obscured between phases ~0.2 to ~0.7. This would require the height of the lowest part of the obscuring matter to be 0.13 to 0.31 times its radius, depending on the actual geometry of the system. If the obscuring matter were in a thick short hollow tube with a height to radius ratio of the unfilled region at its highest point of 0.44 to 1.4, then the soft X-ray peak at $\phi \sim 0.5$ would be explained as due to the accretion region viewed through the hollow part of this obscuring tube.

Obscuration by an ionized electron scattering medium of the same shape could also produce the same soft X-ray light curve. Such a region might exist close to the white dwarf surface, whereas obscuration by non-ionized material is more likely above the shock. These two possibilities would give rise to different medium energy X-ray light curves if the absorbing column of the non-ionized matter was not too high ($5\times10^{20} < N_H <$ few $\times 10^{22}$ in this case). Unfortunately, our ME data are not of sufficient quality for us to comment on this.

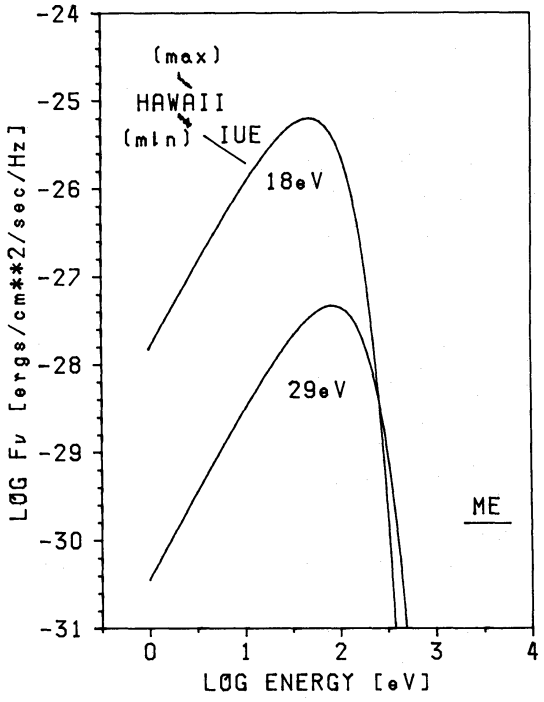

Figure 11. The overall energy distribution of E2003+225 on 1983 October 12. The maximum and minimum optical spectra observed, the best-fit power-law continuum from the *IUE* observations, the two blackbody curves corresponding to the maximum and minimum temperatures allowed by the grating observation and the average of the medium-energy flux observed are shown.

It is also possible that the double-peaked shape of the X-ray light curve could be interpreted in terms of two emitting poles. The circular polarization of N84 allows a second pole to become visible between phases ~0.8 to ~0.1. There are, however, several major difficulties with this hypothesis. The two poles apparently contribute similar fluxes in the soft X-ray band in spite of the fact that they must be viewed at very different inclinations if the magnetic field is dipolar. This requires the pole more distant from the mass-losing star to be intrinsically brighter than the one facing it. At the same time this brighter pole must produce no strong emission lines (the observed radial velocity variation is sinusoidal, the equivalent-width peak does not cover the right phase interval). Some of these arguments do not apply if the two poles are not diametrically opposed, but in this case the second pole must produce very little polarized light despite its soft X-ray luminosity. Another reason for rejecting the two pole hypothesis is the similarity of the soft X-ray light curves of E2005+223 to those of AN UMa and E1405−451. Polarization studies (Brainerd & Lamb 1986, in preparation) of these latter sources derive dipole geometries which do not allow the second pole to appear from the far side of the white dwarf. Finally, the medium energy X-ray light curve, although of low quality, also suggests a single emitting pole.

4.2 CONTINUUM SPECTRUM

The overall continum spectrum (averaged over the orbital cycle) is given in Fig. 11. In the soft X-ray range the blackbody distributions with the maximum and minimum temperatures allowed by the least-squares fits of the grating data are shown. These values and the implied bolometric luminosities of the two X-ray components (normalized to a distance of 100 pc) are listed in Table 7, where the equivalent values for AM Her are also given. Note that although AM Her is at

Table 7. X-ray luminosity balance in AM Her objects observed with X-ray diffraction gratings.

	E2003+225[a]		AM HER[b]	
	best fit	90% conf. interval	best fit	90% conf. interval
kT_{BB}(eV)	25	18-29	46	40-55
$L_{BB}/d^2_{100}(10^{31}$erg.cm^{-2}.s$^{-1})$	13	6.3-79	63	--
$N_H(cm^{-2})$[c]	5.6	3.8-9.4	2.8	0.7-5.6
$L_{TB}/d^2_{100}(10^{31}$erg.cm^{-2}.s$^{-1})$[d]	--	0.8-2.9[e]	49	--

[a] this paper, luminosities evaluated using mean flux and a geometry factor of 4π

[b] Heise et al. 1984, except L_{TB} from Rothschild et al. 1981

[c] derived from soft X-ray grating data

[d] determined for the same time interval as L_{BB}

[e] not derived from a spectral fit

~75 pc (Young & Schneider 1981), E2003+225 is at least 150 pc away (Paper II). The soft X-ray flux (0.1–0.25 keV) observed is 21 per cent of the unabsorbed bolometric flux if $kT_{BB}=29$ eV and 1.7 per cent of this flux if $kT_{BB}=18$ eV, the largest corrections being due to absorption. The hard X-ray flux (2–6 keV) observed is 46–13 per cent of the 1–100 keV flux assuming a thermal bremsstrahlung spectrum with $5<kT_{BB}<60$ keV and no significant absorption. The total luminosity in the blackbody component is higher than that in the thermal bremsstrahlung component by at least a factor of 4.5, but more probably by a factor of 14.

At 100 pc the implied blackbody emitting area is $1.6\pm^{22.4}_{1.2}\times10^{14}$ cm^2, corresponding to a fractional emitting area for a 10^9 cm radius white dwarf of $1.3\pm^{17.7}_{0.96}\times10^{-5}$, which can be compared to the value of 1.1×10^{-5} derived by Heise *et al.* (1984) for AM Her using the *Einstein* OGS.

The average optical and UV emissions are roughly accounted for by a power law of spectral index ~1.1. The luminosity in these components is $\sim10^{32}\,d^2_{100}$ erg s^{-1} in the frequency range 10^{14}–10^{15} Hz.

In the commonly accepted picture for this class of objects (see e.g. Lamb 1985) the medium-energy X-ray emission is attributed to thermal bremsstrahlung from gas below the shock at the base of the accretion funnel, while the soft X-rays derive from the re-radiation by the white dwarf surface of the energy released in the shock region. The infrared and optical radiation is interpreted as cyclotron emission. Other sources of light in the system could be the white dwarf surface, which should be important in the far-UV, and the line-emitting gas which may contribute in the optical band.

The widely discussed imbalance between soft and medium energy X-ray luminosity (e.g. King 1983) is confirmed by this system, although estimates based on photospheric rather than blackbody spectra may ease the problem. It is interesting to note that the optical-UV luminosity is comparable to that in soft X-rays for intermediate values of the temperature. This suggests that the soft X-rays derive from reprocessing of the cyclotron losses, which in this system must exceed bremsstrahlung losses in order to account for the observed soft X-ray flux. The soft X-ray puzzle might not be present in such circumstances.

Acknowledgments

The authors acknowledge the effort of the *EXOSAT* duty scientists in producing the ESOC interactive analysis package and wish to thank Linda Osborne for typing this manuscript. We also thank Drs Tapia and Cropper for providing unpublished material. JPO acknowledges receipt of an ESA fellowship and wishes to thank the Department of Astrophysics, Oxford University, for hospitality whilst preparing this work for publication. KM is a recipient of an Overseas Research Scholarship. GJH and JPH would like to acknowledge the use of spectral reduction programs written by J. W. MacKenty.

References

Andronov, I. L. & Yavorskii, Yu. B., 1983. *Soviet astr. Lett.*, **9,** 291.

Biermann, P., Schmidt, G. D., Liebert, J., Stockman, H. S., Tapia, S., Kühr, H., Strittmatter, P. A., West, S. & Lamb, D. Q., 1985. *Astrophys. J.*, **293,** 303.

Cordova, F. A., Mason, K. O. & Kahn, S. M., 1985. *Mon. Not. R. astr. Soc.*, **212,** 447.

Cropper, M., 1985. *PhD thesis,* University of Cape Town.

de Korte, P. A. J., Bleeker, J. A. M., den Boggende, A. J. F., Branduardi-Raymont, G., Brinkman, A. C., Culhane, J. L., Gronenschild, E. H. B. M., Mason, I. & McKechnie, S. P., 1981. *Space Sci. Rev.*, **30,** 495.

Heise, J., Kruszewski, A., Chlebowski, T., Mewe, R., Kahn, S. & Seward, F. D., 1984. *Phys. Scripta,* **T7,** 115.

Hlivak, R. J., Henry, J. P. & Pilcher, C. B., 1984. In: *Proc. Soc. Photo-Opt. Eng. 445. Instrumentation in Astronomy,* **5,** 122.

Kholopov, P. N., Samus, N. N., Kaznrovets, E. V. & Perova, N. B., 1985. *Inform. Bull. Var. Stars 2681.*

King, A. R., 1983. In: *Cataclysmic Variables and Related Objects,* p. 181, eds Livio, M. & Shaviv, G., Reidel, Dordrecht, Holland.

King, A. R. & Williams, G. A., 1985. *Mon. Not. R. astr. Soc.*, **215,** 1P.

Lamb, D. Q., 1985. In: *Cataclysmic Variables and Low Mass X-ray Binaries,* p. 179, eds Patterson, J. & Lamb, D. Q., Reidel, Dordrecht, Holland.

Liebert, J. & Stockman, H. S., 1985. In: *Cataclysmic Variables and Low Mass X-ray Binaries,* p. 151, eds Patterson, J. & Lamb, D. Q., Reidel, Dordrecht, Holland.

Imamura, J. N. & Durisen, R. H., 1983. *Astrophys. J.*, **268,** 291.

Miller, J. S., Robinson, L. B. & Wampler, E. J., 1976. *Advances in Electronics and Electron Physics,* **40B,** 693, Academic Press, New York.

Mukai, K., Bonnet-Bidaud, J. M., Charles, P. A., Corbet, R. H. D., Maraschi, L., Osborne, J. P., Smale, A. P., Treves, A., Van der Klis, M. & van Paradijs, J., 1986. *Mon. Not. R. astr. Soc.*, submitted, (Paper 2).

Nousek, J. A., Luppino, G., Gajor, S., Bond, H. E., Grauer, A. D., Schmidt, G., Hill, G. & Tapia, S., 1982. *IAU Circ 3733.*

Nousek, J. A., Takalo, L. O., Schmidt, G. D., Tapia, S., Hill, G. J., Bond, H. E., Grauer, A. D., Stern, R. A. & Agrawal, P. C., 1984. *Astrophys. J.*, **277,** 682, (N84).

Nugent, J. J., Jensen, K. A., Nousek, J. A., Garmire, G. P., Mason, K. O., Walter, F. M., Bowyer, C. S., Stern, R. A. & Riegler, G. R., 1983. *Astrophys. J. Suppl.*, **51,** 1.

Osborne, J. P. *et al.*, 1984. In: *X-Ray Astronomy '84,* p. 59, eds Oda, M. & Giacconi, R., Institute of Space and Aeronautical Science, Tokyo.

Osborne, J. P., 1985. *EXOSAT Express,* **13,** 42.

Paresce, F., 1984. *Astr. J.*, **89,** 1022.

Robinson, L. B. & Wampler, E. J., 1972. *Publs astr. Soc. Pacif.*, **84,** 161.

Rothschild, R. E., Gruber, D. E., Knight, F. K., Matteson, J. L., Nolan, P. L., Swank, J. H., Holt, S. S., Serlemitsos, P. J., Mason, K. O. & Tuohy, I. R., 1981. *Astrophys. J.*, **250,** 732.

Stone, R. P. S., 1977. *Astrophys. J.*, **218,** 767.

Turner, M. J. L., Smith, A. & Zimmerman, H. U., 1981. *Space Sci. Rev.*, **30,** 513.

Young, P. & Schneider, D. P., 1981. *Astrophys. J.*, **247,** 960.